

Lasers in Manufacturing Conference 2021

# Optical system for multi Bessel beam high power ultrashort pulsed laser processing using a spatial light modulator

Christian Lutz<sup>a\*</sup>, Simon Schwarz<sup>a</sup>, Stefan Rung<sup>a</sup>, Jan Marx<sup>b</sup>, Cemal Esen<sup>b</sup>, Ralf Hellmann<sup>a</sup>

<sup>a</sup>University of Applied Science Aschaffenburg, Würzburgerstraße 45, 63743 Aschaffenburg, Germany

<sup>b</sup>Ruhr University Bochum, Universitätsstraße 150, 44801 Bochum, Germany

---

## Abstract

We report on an optical setup for multi Bessel beam processing combining a refractive axicon and a spatial light modulator. Based on their particular beam profile, Bessel beams exhibit various advantages over conventional Gaussian beams for ultrashort pulsed laser processing. Especially for micromachining of transparent materials, applications such as micro-hole drilling or the generation of voids benefit from the increased focal length of the applied Bessel beam. In addition, on account of the significantly increased average output power of industrial ultrashort pulsed lasers over the last years, there is a high demand on multi spot applications for using the available laser power in efficient production processes. Our optical concept combines the dynamic possibilities of beam splitting using spatial light modulator with the benefits of Bessel beams facilitating multi Bessel beam processing.

Keywords: Bessel beam; axicon; optical system; ultrashort pulsed laser; material ablation

---

## 1. Introduction

Diffraction-free Bessel beams, first discovered and described by Durnin et al. [1] in 1987, are the propagation-invariant solutions of the Helmholtz equation. While Durnin et al. [2] showed convergences to the ideal Bessel beams for a finite range, in theory they are of infinite transverse extent and carry infinite energy, so they cannot be generated experimentally [3; 4]. To design so-called a quasi-Bessel beam, based from a Gaussian beam profile, there are some commonly used components like apertures [2], binary-coded holograms [5], axicon lenses [6], converging lenses with spherical aberrations [7], tunable acoustic gradient lenses [8] and spatial light modulators [9]. Based on their specific intensity distribution, quasi-Bessel beams have advantages for different micro machining processes. Especially for drilling holes with higher aspect ratios, quasi-Bessel beams are an outstanding tool because of the long high intensity range in propagation direction. In view of this benefit, Xie et al. [4] showed Bessel beam drilling experiments with 52 times larger aspect ratio than that formed by using Gaussian beams in similar focusing conditions. By optimizing the focal position and

the pulse energy they reached an aspect ratio up to 330:1 in PMMA for holes with a diameter between 1.5  $\mu\text{m}$  and 2.4  $\mu\text{m}$ . Using an pulse energy of 2mJ, Dudutis et al. [10] produced intra-volume modifications in soda glass with a maximum length of approximately 2.3 mm for generating cracks in axial direction induced from the elliptical shape of the central core diameter. Finally, they demonstrated the possibility to control the crack orientation by rotating the Bessel beam profile around the propagation axis. Furthermore, Mitra et al. [11] fabricated nanovoids up to 5 mm in length in borosilicate glass, corresponding to an aspect ratio of 1200:1. For non-transparent materials, the aspect ratios of drilled microholes are much smaller using Bessel beams, as Alexeev et al. [12] demonstrated in a 100  $\mu\text{m}$  copper sheet with holes having an exit diameter of 15  $\mu\text{m}$ . Indeed, on the entrance of the drilled holes circular material modifications appear due to the typical Bessel beam intensity distribution. To minimize these effects, He et al. [13] developed a tailored Bessel beam by using a binary phase plate in front of the axicon. Due to this tailored Bessel beam, the modification of the upper surface is minimized and enables drilling of 6  $\mu\text{m}$  holes in a 100  $\mu\text{m}$  silicon wafer. Spatial light modulators are varied optical elements for a lot of different beam shaping applications like spherical aberration correction [14] and multisport processing [15]. Due to the limited phase modification of a spatial light modulator (SLM), the accessible corresponding axicon angles are still small, resulting in long Bessel beams of many centimeters or meters in length [16]. Also the generation of Bessel beam arrays are a promising method for drilling applications with multi spot beam profiles [17]. Contrary to conventional axicons generating one quasi-Bessel

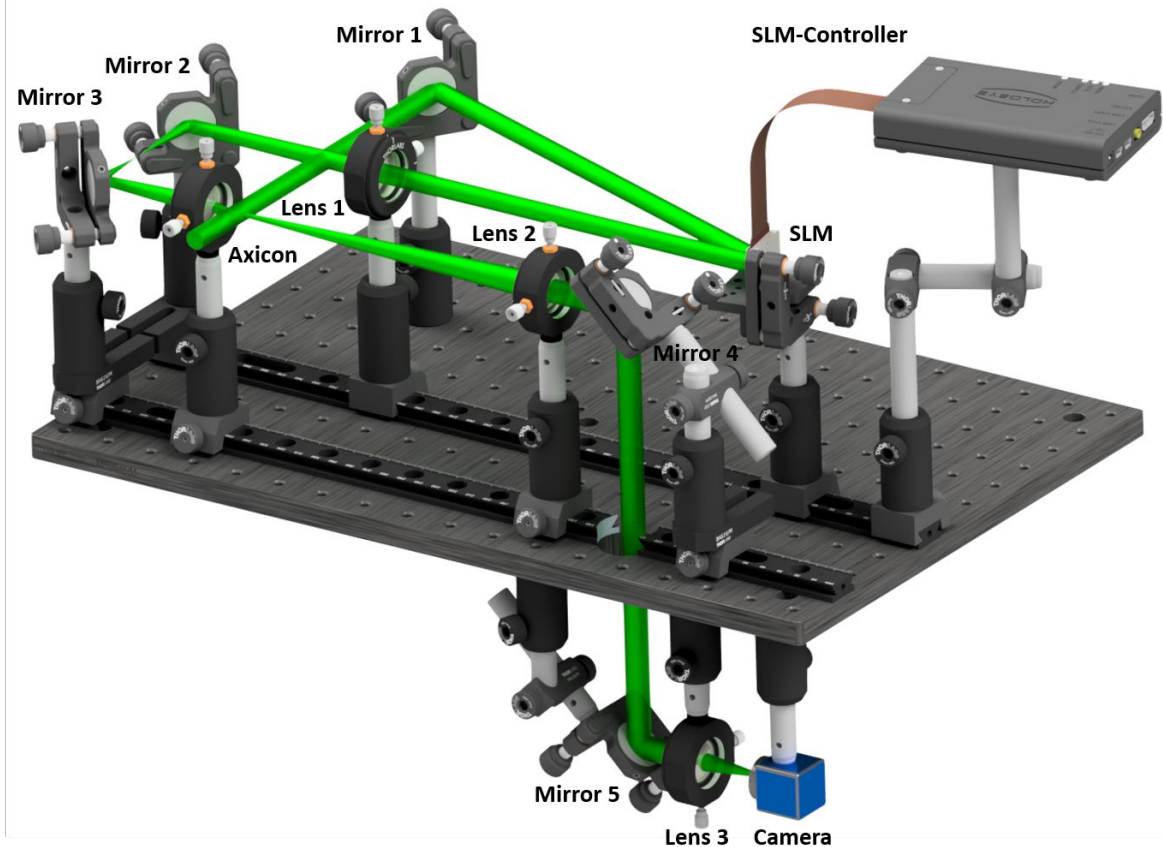


Fig. 1 Schematic illustration of the optical system for multi Bessel beam generation using a spatial light modulator (SLM), a 4f telescope, an axicon, a focusing lens and a camera for the beam profile detection.

beam behind their apex, axicon arrays can be used to form a multitude of these beams. Schwarz et al. [18] showed femtosecond laser ablation processing for micro axicon arrays including a characterization of the resulting multi-Bessel beams. While the axicon angle realizable with a SLM, because of the limited phase shift per pixel, is quite small, often too large Bessel beams result. Based on that, we demonstrate an optical setup, depicted in Fig. 1, which combines the flexible beam splitting possibilities of a SLM, with useful axicon angles for multi Bessel beam shaping.

## 2. Experimental

We used an ultrashort pulsed laser (Light Conversion, Pharos) with a wavelength of 1028 nm, an adjustable repetition rate up to 610 kHz and with a pulse duration between 230 fs and 15 ps. By using the second harmonic of the fundamental, a wavelength of 514 nm can be emitted having the same pulse duration and repetition rate. The linear polarized laser beam is shaped by a Holoeye SLM with a resolution of 1920x1080 pixels (Pluto 2, VIS016) in combination with a 170° precision axicon from Eksma Optics and different lenses, to complete the optical setup. After reflecting the laser beam from the SLM, the first lens ( $f=100$  mm) is placed 200 mm behind the SLM to image its phase pattern into the following axicon. Behind the axicon, the resulting Bessel beam is imaged by a 4f setup with two lenses with  $f=100$  mm and  $f=150$  mm into the focal plane. By superimposing the phase pattern of the SLM and the imaged Bessel beam, multi Bessel beam results in the focus of lens 3. To image the intensity distribution, a camera (IDS UI149xSE-M) is used, which can be replaced by a workpiece in order to experimental drilling applications. With this optical setup which is also shown in Fig. 1, it is possible to adjust the separation in a multi spot beam profile by using the SLM with different beam splitter patterns and generate multi Bessel beams with the included axicon. To simulate parameters like the spot separation and the axicon angle, Lighttrans Virtual Lab is used.

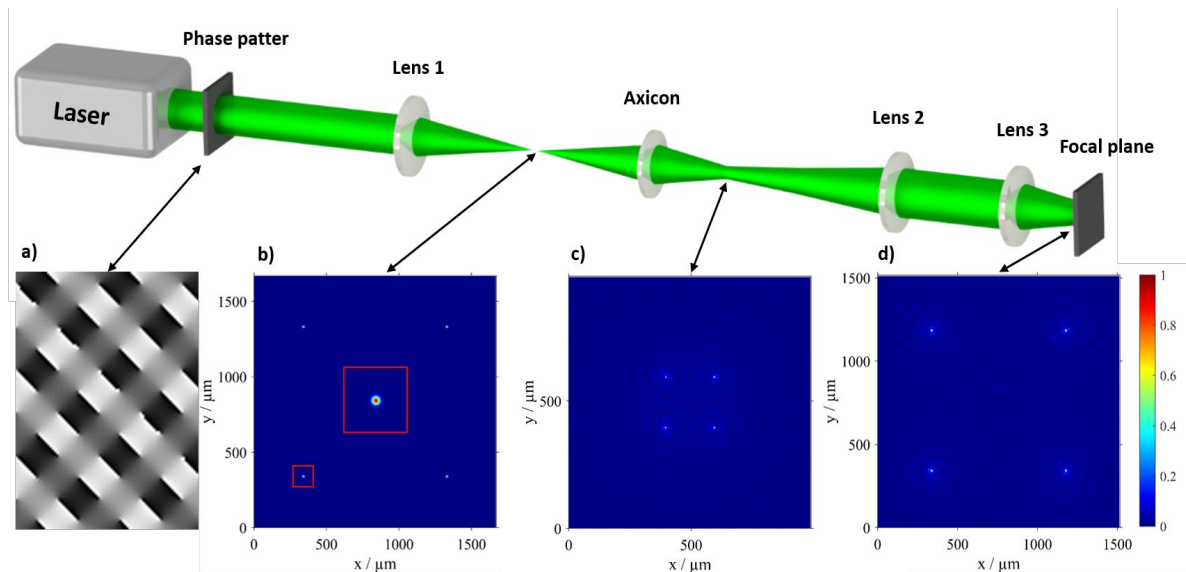


Fig. 2 Schematic illustration of the simulated beam path including a SLM with a 4f-telescope and an axicon with a following imaging setup. Different phase patterns showing a varied spot separation in the focal plane and raising diffraction effects for smaller separations.

### 3. Results

The simulation results in Fig. 2 show an optical system to generate multi Bessel beams with the described combination of a spatial light modulator and an axicon. The input beam is defined with 3.4 mm in diameter ( $1/e^2$ ) with a Gaussian shape, which is directed on the SLM. The phase pattern Fig. 2a) is a computer-generated hologram (CGH), calculated with an iterative Fourier transform algorithm with a spot separation of 1 mm for a focal length of 100 mm. Thus, at the focal plane between lens 1 and the following axicon, Fig.2b) shows a 2x2 regular beam splitter with Gaussian shaped spots and a separation of 1 mm. As a result of the superposition of the phase pattern, in 30 mm distance from the axicon a multiplied Bessel beam with a separation of 200  $\mu\text{m}$  is shown in Fig.2c). Through the following two lenses the beam profile is imaged into the focal plane with a separation of 1 mm, where material processing is possible. As shown in Fig. 1, based on the simulation results we transfer the optical setup to an optical breadboard to realize module integration into an existing USP-laser machine. For the evaluation of the optical simulation, we measured the beam profiles at characteristic positions along the beam path with an IDS camera in accordance with Fig. 2. The Gaussian input beam Fig. 3e) with a diameter of 3.4 mm results in a beam splitter with 1 mm separation, matching with the simulation. In addition, the multi Bessel beam Fig. 3f) detected 30 mm behind the axicon shows the same dimensions as in Fig. 2c), which reflects the correspondence between the simulation and the experimental setup. While Fig. 3g) illustrates the multi Bessel beam resulting 30 mm after lens 3, Fig. 3h) shows one of the Bessel beams in larger dimensions with the typical high intensity peak and ring shaped profiles around it. Both, in simulation and in experimental setup diffraction effects occur from the superposition of the SLM phase pattern and the axicon. Also Orlov et al. [17] reported these interferences surrounding the nearby beams. If we remove the computer-generated hologram (CGH) and use the SLM as a mirror, the single resulting Bessel beam does not show these effects. Another effect is the visibility of the zeroth order in the center of the beam profile, which does not occur in the simulation results as an ideal diffraction element is used.

In Fig. 4 we illustrate the lateral intensity distributions of the multi Bessel beam in the focal plane for different distances from lens 3. Slices along the z-axis illustrate a slightly increasing separation of the Bessel beams with a maximum of approximately 300  $\mu\text{m}$ . It is found that with increasing distance, more intensity is visible in the background surrounding the degrading Bessel beams. Due to data analyzing, we found a decreasing high intensity peak for an increasing distance from the focal plane, what is not visible in the magnification in Fig. 4 because of normalized scale. Compared to other optical setups for multi Bessel beams with a fixed spot separation [18], we have a variable setup. Contrary to other setups using microscope objectives to decrease the size of the Bessel beam [17; 13], we demonstrated the multi Bessel beam generation being applicable for the use with galvanometer scanner systems.

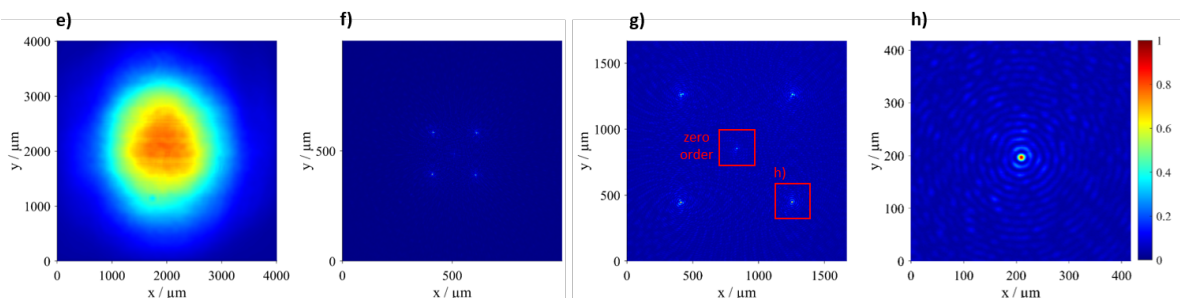


Fig. 3 Measured lateral intensity distributions of the input beam e), the multi Bessel beam 30 mm behind the axicon f), the multi Bessel Beam in the focal plane of Lens 3 g) and an enlarged partial beam h).

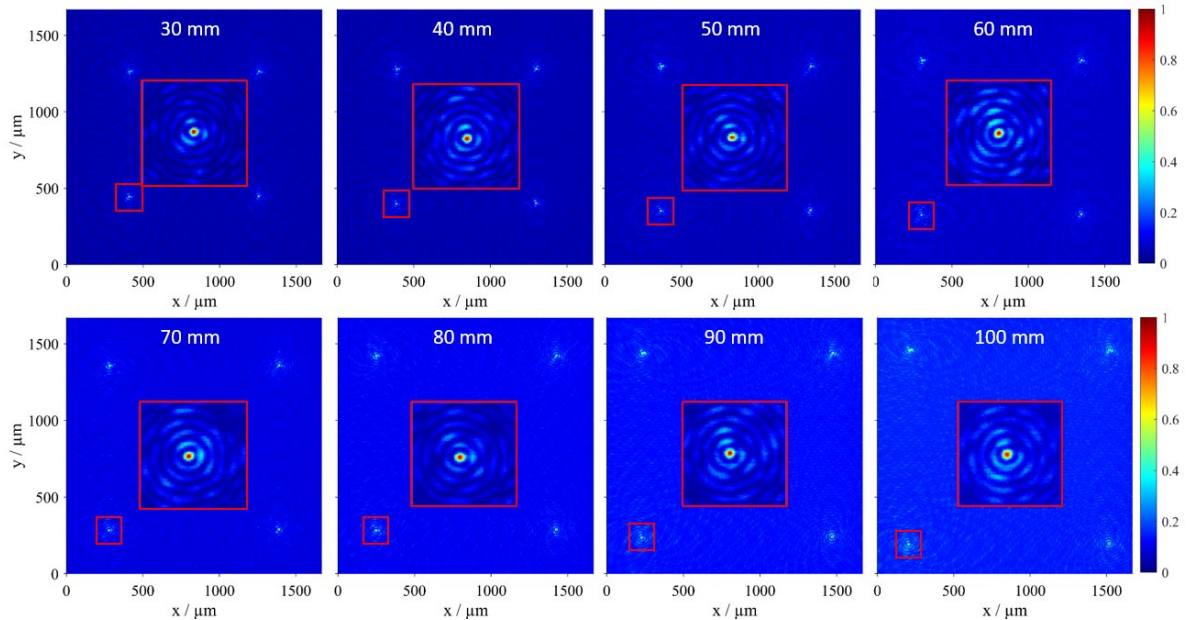


Fig. 4 Measured lateral intensity distributions of the multi Bessel beam in the focal plane after Lens 3 taken in different z-axis positions from 30 mm to 100 mm in 10 mm steps.

#### 4. Conclusion

We have demonstrated an optical system for multi Bessel beam generation using a spatial light modulator and an axicon lens. Distinguished agreement between simulated and experimentally determined beam profiles at selected positions along the beam path is highlighted. The presented multi Bessel beams have a spot separation of 1 mm in 30 mm distance from lens 3 while showing little interference surrounding the single beams. The setup combines the flexibility of spot separation using customized phase patterns and the possibility of larger axicon angles to generate small high intensity Bessel beams. The results demonstrate the opportunity for scanning based material processing using multi Bessel beams for higher throughput in drilling applications.

#### References

- [1] J. Durnin: J. Opt. Soc. Am. A, 4, (1987) 4.
- [2] J. Durnin, J. Miceli and J. Eberly: Phys. Rev. Lett., 58, (1987) 15.
- [3] O. Brzobohatý, T. Cizmár and P. Zemánek: Opt. Express, 16, (2008) 17.
- [4] Q. Xie, X. Li, L. Jiang, B. Xia, X. Yan, W. Zhao and Y. Lu: Appl. Phys. A, 122, (2016) 2.
- [5] S. K. Tiwari, S. R. Mishra, S. P. Ram and H. S. Rawat: Appl Opt, 51, (2012) 17.
- [6] S. Schwarz, S. Rung, C. Esen and R. Hellmann: Opt. Express, 26, (2018) 18.
- [7] H. Zhang: Opt. Commun., 39, (2000) 3.
- [8] E. McLeod, A. B. Hopkins and C. B. Arnold: Opt. Lett., 31, (2006) 21.
- [9] N. Chattapiban, E. A. Rogers, D. Cofield, W. T. Hill and R. Roy: Opt. Lett., 28, (2003) 22.
- [10] J. Dudutis, P. Gečys and G. Račiukaitis: Opt. Express, 24, (2016) 25.
- [11] S. Mitra, M. Chanal, R. Clady, A. Mouskeftaras and D. Grojo: Appl Opt, 54, (2015) 24.
- [12] I. Alexeev, K.-H. Leitz, A. Otto and M. Schmidt: Phys. Procedia., (2010) 5.

- [13] F. He, J. Yu, Y. Tan, W. Chu, C. Zhou, Y. Cheng and K. Sugioka: *Sci. Rep.*, (2017) 7.
- [14] G.-L. Roth, S. Rung, C. Esen and R. Hellmann: *Opt. Express*, 28, (2020) 4.
- [15] C. Lutz, G. Roth, S. Rung, C. Esen, R. Hellmann: *J. Laser Micro Nanoeng.*, (2021) 16.
- [16] I. A. Litvin, T. Mhlanga and A. Forbes: *Opt. Express*, 23, (2015) 6.
- [17] Sergej Orlov, Alfonsas Juršėnas, Justas Baltrukonis and Vytautas Jukna: *J. Laser Micro Nanoeng.*, (2018) 13.
- [18] S. Schwarz, S. Rung, C. Esen and R. Hellmann: *J Laser Appl.*, 32, (2020) 1.